ELSEVIER

Journal of Alloys and Compounds 404–406 (2005) 657–660

Journal of ALLOYS AND COMPOUNDS

www.elsevier.com/locate/jallcom

Phase structures and electrochemical performance of $V_{2.1}TiNi_{0.5}Hf_{0.05}Co_x$ ($x = 0$–0.192) hydrogen storage alloys

L.X. Chen*, R. Guo, Y.Q. Lei, F.B. Dai, L. Li, B. Liao, C.P. Chen, Q.D. Wang

Department of Materials Science and Engineering, Zhejiang University, Hangzhou 310027, PR China

Received 1 June 2004; received in revised form 2 September 2004; accepted 15 September 2004
Available online 7 July 2005

Abstract

The phase structures and electrochemical performance of $V_{2.1}TiNi_{0.5}Hf_{0.05}Co_x$ ($x = 0, 0.113, 0.152$ and 0.192) alloys have been investigated. It is found that the addition of Co into the $V_{2.1}TiNi_{0.5}Hf_{0.05}$ alloy decreases the amount of the V-based solid solution main phase and increases the amount of C14-type secondary phase without any change in the pattern of the three-dimensional network structure. With increasing Co content, the unit cell of the main phase contracts and that of the secondary phase expands. Electrochemical measurements show that the maximum discharge capacity of the Co-added alloys is much less than that of $V_{2.1}TiNi_{0.5}Hf_{0.05}$ alloy, but their high-rate dischargeability and cycle stability are markedly improved.

Keywords: Hydrogen storage materials; Phase structures; Electrochemical properties; V-based solid solution; Laves phase

1. Introduction

Since Tsukahara et al. [1,2] reported the novel dual phase hydride electrode alloy $V_3TiNi_{0.56}$, vanadium-based solid solution alloys containing titanium and nickel have been attractive for their potential application in the Ni–MH battery because of their high hydrogen storage capacity. However, the poor cycle stability of these alloys in KOH electrolyte keeps them from being industrialized. Tsukahara et al. [3,4] and Zhang et al. [5–7] investigated the influence of various additive elements to $V_3TiNi_{0.56}$ and $V_3TiNi_{0.56}Hf_{0.24}$ alloys for improving their electrochemical properties, especially, the cycling stability. Their works have shown that multi-component alloying is an effective method for improving the overall properties of these alloys. $V_{2.1}TiNi_x$ ($x = 0.1$–0.9) and $V_{2.1}TiNi_{0.5}Hf_x$ ($x = 0$–0.25) alloys have been studied and reported in our previous works [8,9]. $V_{2.1}TiNi_{0.5}Hf_{0.05}$ was found to have a high discharge capacity of 444 mAh/g and a poor capacity retention of 27.66% after 30 cycles. In order to improve its electrochemical properties further, we chose Co as the added alloying element to inhibit the corrosion of the alloy in KOH electrolyte [10]. The phase structures and electrochemical behaviors of $V_{2.1}TiNi_{0.5}Hf_{0.05}Co_x$ ($x = 0$–0.192) alloys are reported in this paper.

2. Experimental details

All samples of $V_{2.1}TiNi_{0.5}Hf_{0.05}Co_x$ ($x = 0, 0.113, 0.152$ and 0.192) were prepared by vacuum induction melting under argon atmosphere, and each batch was remelted three times to ensure high homogeneity. The metallographic microstructures were examined by using a scanning electron microscopy (SEM) and the chemical compositions determined with an energy dispersive X-ray spectrometer (EDS). Samples were pulverized by first hydriding and then crushed mechanically into a powder of 300 mesh after dehydriding. The crystal structures and lattice parameters were determined by X-ray powder diffraction (XRD) using Cu Kα radiation. The pressure–composition isotherms (*P–C–T* curves) were measured with the electrochemical method. Each test electrode was prepared by mixing alloy powder with copper powder in the weight ratio of 1:2 and then cold-pressed the mixture into a pellet. The electrochemical properties of

* Corresponding author. Tel. +86 571 8795 1152; fax: +86 571 8795 1152.
E-mail address: lxchen@zju.edu.cn (L.X. Chen).

0925-8388/$ – see front matter © 2005 Elsevier B.V. All rights reserved.
doi:10.1016/j.jallcom.2004.09.085

these negative electrodes were measured in a tri-electrode open cell at 298 K with a sintered $Ni(OH)_2$/NiOOH positive counter electrode and a Hg/HgO reference electrode. The negative electrodes were charged at 100 mA/g for 6.5 h and discharged at 25–500 mA/g to the cutoff potential of −0.70 V versus Hg/HgO. The exchange current densities I_o of alloys were calculated from the slopes of micropolarization curves, which were determined by scanning the electrode potential at 0.1 mV/s from −5 to 5 mV (versus open-circuit potential) with a Solartron SII287 potentiostat.

3. Results and discussion

3.1. Phase structures

The XRD patterns of the $V_{2.1}TiNi_{0.5}Hf_{0.05}Co_x$ ($x = 0$–0.192) alloys are shown in Fig. 1. All alloys consist of two phases indexed as a main phase of V-based solid solution with b.c.c. structure and a secondary phase of C14-type Laves phase. The calculated lattice parameters of each phase are shown in Table 1. It can be seen that the lattice parameter of the main phase decreases from 0.30626 to 0.30507 nm, and those of the secondary phase significantly increase with increasing Co content from $x = 0$ to 0.192.

The SEM micrographs of the $V_{2.1}TiNi_{0.5}Hf_{0.05}Co_x$ ($x =$ 0–0.192) alloys are shown in Fig. 2. It can be seen that the secondary phase precipitates along the grain boundaries of the main phase in the form of a three-dimensional network. With the increase of Co content, the grain size of the main phase decreases. Based on the compositions determined by the EDS analysis, the molar fractions of the main and secondary phases are calculated [11] and shown in Table 1. It can be seen that the increase of Co content gives rise to a decrease of the amount of the main phase and an increase of the amount of the secondary phase, which is in good agreement with SEM observation. In addition, only a small portion of Co goes into the V-based solid solution and the main portion of it stays in the secondary phase together with Hf and Ni, leading to the increase of the amount of the secondary phase.

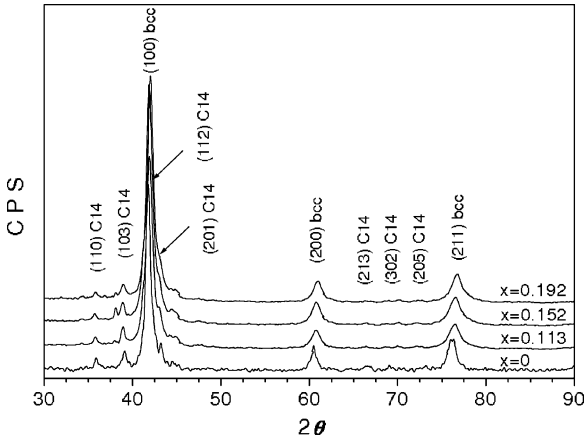

Fig. 1. XRD patterns of $V_{2.1}TiNi_{0.5}Hf_{0.05}Co_x$ ($x = 0$–0.192) alloys.

3.2. Electrochemical properties

The maximum discharge capacities of the $V_{2.1}TiNi_{0.5}Hf_{0.05}Co_x$ ($x = 0$–0.192) alloys are shown in Fig. 3. It can be seen that $V_{2.1}TiNi_{0.5}Hf_{0.05}$ has the highest discharge capacity of 444 mAh/g, much higher than that of $V_{2.1}TiNi_{0.5}Hf_{0.05}Co_{0.113}$ alloy (386 mAh/g). When increasing the Co content further to $x = 0.152$–0.192, the maximum discharge capacity decreases to 329–350 mAh/g. The electrochemical *P–C* isotherms of the above alloys (Fig. 4) indicate that the plateau pressure of the *P–C* isotherms rises and the width of pressure plateau reduces with increasing Co content. We believe that the decrease of the discharge capacity due to the Co addition could be ascribed to two factors: the decrease of the molar fractions and the lattice parameters of the main phase. The former is mainly responsible for the first noticeable decrease (from 444 to 386 mAh/g) while the later is more responsible for the second one (from 386 to 329–350 mAh/g), because comparing with $V_{2.1}TiNi_{0.5}Hf_{0.05}$ and $V_{2.1}TiNi_{0.5}Hf_{0.05}Co_{0.113}$, the equilibrium hydrogen pressure of $V_{2.1}TiNi_{0.5}Hf_{0.05}Co_{0.152}$ or $V_{2.1}TiNi_{0.5}Hf_{0.05}Co_{0.192}$ is almost the same and distinctly higher, as a smaller cell volume generally leads to a higher equilibrium pressure.

Fig. 5 shows the relations between discharge capacity and discharge current density for the $V_{2.1}TiNi_{0.5}Hf_{0.05}Co_x$ ($x =$ 0–0.192) alloys. At larger discharge current densities (400–

Table 1
The characteristics of the phase structures in the$V_{2.1}TiNi_{0.5}Hf_{0.05}Co_x$ ($x = 0$–0.192) alloys

x	Phase	Composition (at.%)					Molar fraction	Lattice parameters (nm)
		V	Ti	Ni	Hf	Co		
0	Main phase	75.23	19.44	5.28	0.04	–	0.69	$a = 0.30626$
	Secondary phase	15.98	44.51	36.01	3.50	–	0.31	$a = 0.50147$, $c = 0.80933$
0.113	Main phase	76.09	16.84	4.88	0.67	1.52	0.58	$a = 0.30536$
	Secondary phase	25.32	42.19	25.74	2.53	4.22	0.42	$a = 0.50163$, $c = 0.82497$
0.152	Main phase	77.50	15.41	4.31	0.16	2.62	0.53	$a = 0.30526$
	Secondary phase	31.62	39.53	20.16	2.37	6.32	0.47	$a = 0.50199$, $c = 0.82106$
0.192	Main phase	78.13	14.39	4.17	0	4.32	0.49	$a = 0.30507$
	Secondary phase	35.71	37.59	15.41	2.26	9.02	0.51	$a = 0.50145$, $c = 0.82128$

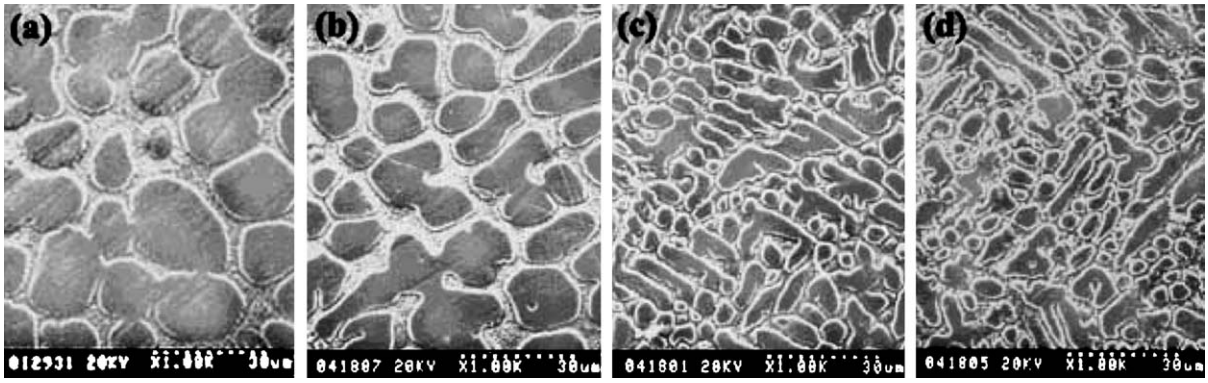

Fig. 2. Scanning electron micrographs of $V_{2.1}TiNi_{0.5}Hf_{0.05}Co_x$ ($x = 0$–0.192) alloys: (a) $x = 0$; (b) $x = 0.113$; (c) $x = 0.152$; (d) $x = 0.192$.

500 mA/g), the discharge capacities of the Co-added alloys are much higher than that of $V_{2.1}TiNi_{0.5}Hf_{0.05}$. From the high-rate dischargeability (HRD_{400}) of these alloys at the discharge current density of 400 mA/g shown in Table 2, it can be seen that $V_{2.1}TiNi_{0.5}Hf_{0.05}Co_{0.192}$ has the best high-rate dischargeability (HRD_{400} of 50.15%) among the alloys studied. These results are also supported by the magnitude of the exchange current densities I_o (Table 2) calculated from the slopes of micropolarization curves of the alloys.

The cycling capacity degradation curves of the $V_{2.1}TiNi_{0.5}Hf_{0.05}Co_x$ ($x = 0$–0.192) alloys are shown in Fig. 6. All of the alloys were activated within six charge–discharge cycles. The discharge capacity of $V_{2.1}TiNi_{0.5}Hf_{0.05}$ reduces rapidly and its capacity retention after 30 cycles is only 27.66%. However, the degradation of the Co-added alloy slows down with increasing Co content. For example, the capacity retention of $V_{2.1}TiNi_{0.5}Hf_{0.05}Co_{0.192}$ is 87.32% after 30 cycles and 46.02% after 100 cycles, much better than that of $V_{2.1}TiNi_{0.5}Hf_{0.05}$. These indicate that the addition of Co is helpful in improving the cycling stability of the $V_{2.1}TiNi_{0.5}Hf_{0.05}Co_x$ alloys. Although the dissolution of vanadium in the alloy into KOH electrolyte is fast, Co

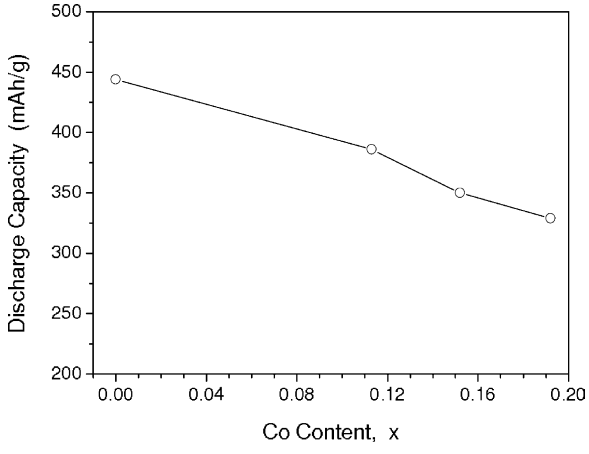

Fig. 3. The maximum discharge capacity of $V_{2.1}TiNi_{0.5}Hf_{0.05}Co_x$ ($x = 0$–0.192) alloys charged at 100 mA/g and discharged at 25 mA/g.

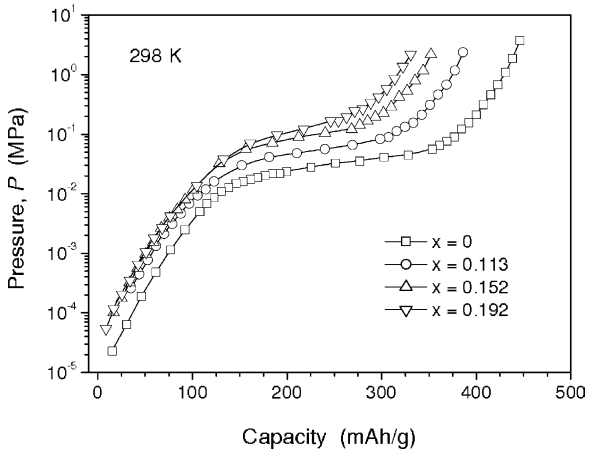

Fig. 4. The electrochemical hydrogen desorption P–C isotherms of $V_{2.1}TiNi_{0.5}Hf_{0.05}Co_x$ ($x = 0$–0.192) alloys at 298 K.

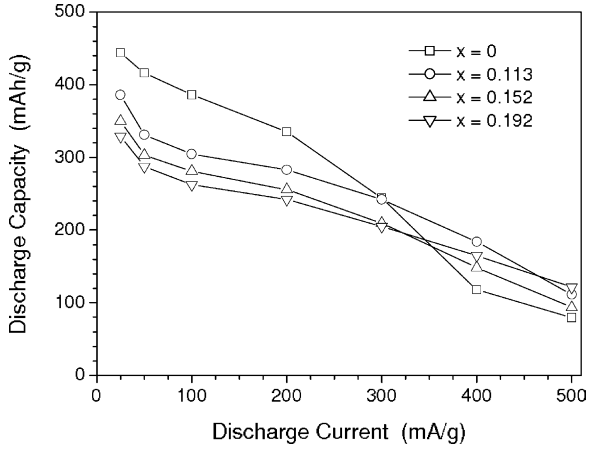

Fig. 5. Relations between discharge capacity and discharge current for $V_{2.1}TiNi_{0.5}Hf_{0.05}Co_x$ ($x = 0$–0.192) alloys.

Table 2
The high-rate dischargeability ($HRD_{400} = C_{400}/C_{25} \times 100\%$) and exchange current densities I_o of $V_{2.1}TiNi_{0.5}Hf_{0.05}Co_x$ ($x = 0$–0.192) alloys

x	0	0.113	0.152	0.192
HRD_{400} (%)	26.50	47.60	42.37	50.15
I_o (mA/g)	96.14	107.8	96.90	131.0

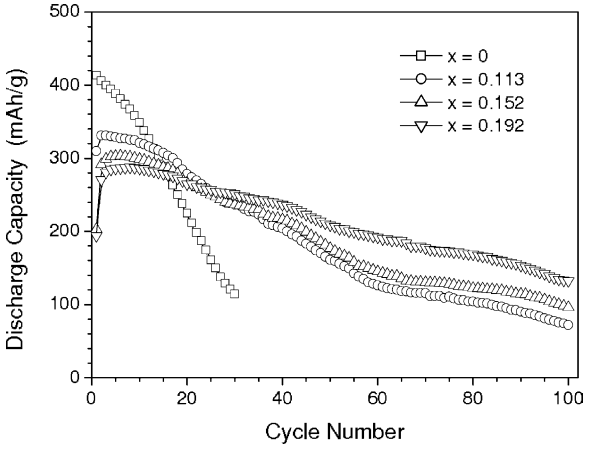

Fig. 6. The cycling capacity degradation curves of $V_{2.1}TiNi_{0.5}Hf_{0.05}Co_x$ ($x = 0$–0.192) alloys charged at 100 mA/g and discharged at 50 mA/g.

restricts the dissolution of vanadium and improves the corrosion resistance of this series alloys in KOH electrolyte solution noticeably [10].

4. Conclusions

All of the $V_{2.1}TiNi_{0.5}Hf_{0.05}Co_x$ ($x = 0$–0.192) alloys consist of two phases indexed as a main phase of V-based solid solution with b.c.c. structure and a secondary phase of C14-type Laves phase. The C14 Laves phase precipitates along the grain boundaries of the main phase in the form of a three-dimensional network. After adding Co, the unit cell of the main phase contracts and that of the secondary phase expands.

The maximum discharge capacity of the Co-added alloys is much less than that of the $V_{2.1}TiNi_{0.5}Hf_{0.05}$ alloy. The decrease of the molar fractions and the lattice parameters of the main phase are thought to be the main reasons. On the other hand, the addition of Co into the $V_{2.1}TiNi_{0.5}Hf_{0.05}$ alloy is significantly beneficial for the high-rate dischargeability and the cycling stability.

Acknowledgements

The authors wish to express their gratitude and appreciation for the support from The National Natural Science Foundation of China (No. 50271064) and The National High Technology Research and Development Program of China (No. 2003AA515021).

References

[1] M. Tsukahara, K. Takahashi, T. Mishima, T. Sakai, H. Miyamura, N. Kuriyama, I. Uehara, J. Alloys Compd. 224 (1995) 162.
[2] M. Tsukahara, K. Takahashi, T. Mishima, T. Sakai, H. Miyamura, N. Kuriyama, I. Uehara, J. Alloys Compd. 226 (1995) 203.
[3] M. Tsukahara, K. Takahashi, T. Mishima, A. Isomura, T. Sakai, J. Alloys Compd. 245 (1996) 59.
[4] M. Tsukahara, K. Takahashi, A. Isomura, T. Sakai, J. Alloys Compd. 287 (1999) 215.
[5] Q.A. Zhang, Y.Q. Lei, L.X. Chen, Q.D. Wang, Mater. Chem. Phys. 71 (2001) 58.
[6] Q.A. Zhang, Y.Q. Lei, X.G. Yang, Y.L. Du, Q.D. Wang, J. Alloys Compd. 296 (2000) 87.
[7] Q.A. Zhang, Y.Q. Lei, X.G. Yang, Y.L. Du, Q.D. Wang, Int. J. Hydrogen Energy 25 (2000) 977.
[8] R. Guo, L.X. Chen, Y.Q. Lei, B. Liao, T. Ying, Q.D. Wang, Int. J. Hydrogen Energy 28 (2003) 803.
[9] R. Guo, L.X. Chen, Y.Q. Lei, B. Liao, Y.W. Zeng, Q.D. Wang, J. Alloys Compd. 352 (2003) 270.
[10] M. Tsukahara, K. Takahashi, T. Mishima, A. Isomura, T. Sakai, J. Alloys Compd. 253 (1997) 583.
[11] M. Tsukahara, K. Takahashi, T. Mishima, A. Isomura, T. Sakai, J. Alloys Compd. 236 (1996) 151.